

Near-Earth and small main-belt binary asteroids, their population and properties

P. Pravec and P. Scheirich

Astronomical Institute AS CR, Ondřejov, Czech Republic

*Workshop “Solar System science before and after Gaia”
Pisa, Italy, 2011 May 4-6*

Contents

1. Small asteroids as cohesionless structures
2. Binary systems among NEAs and small MBAs – Observations
3. Binary systems among NEAs and small MBAs – Population and properties
4. Asteroid pairs among small MBAs
5. Gaia's astrometric detection of binary asteroids with Photocenter variation
6. Conclusions on Gaia's performance for binary asteroids

Asteroids with sizes 0.2-10 km

– cohesionless bodies, easily breakable

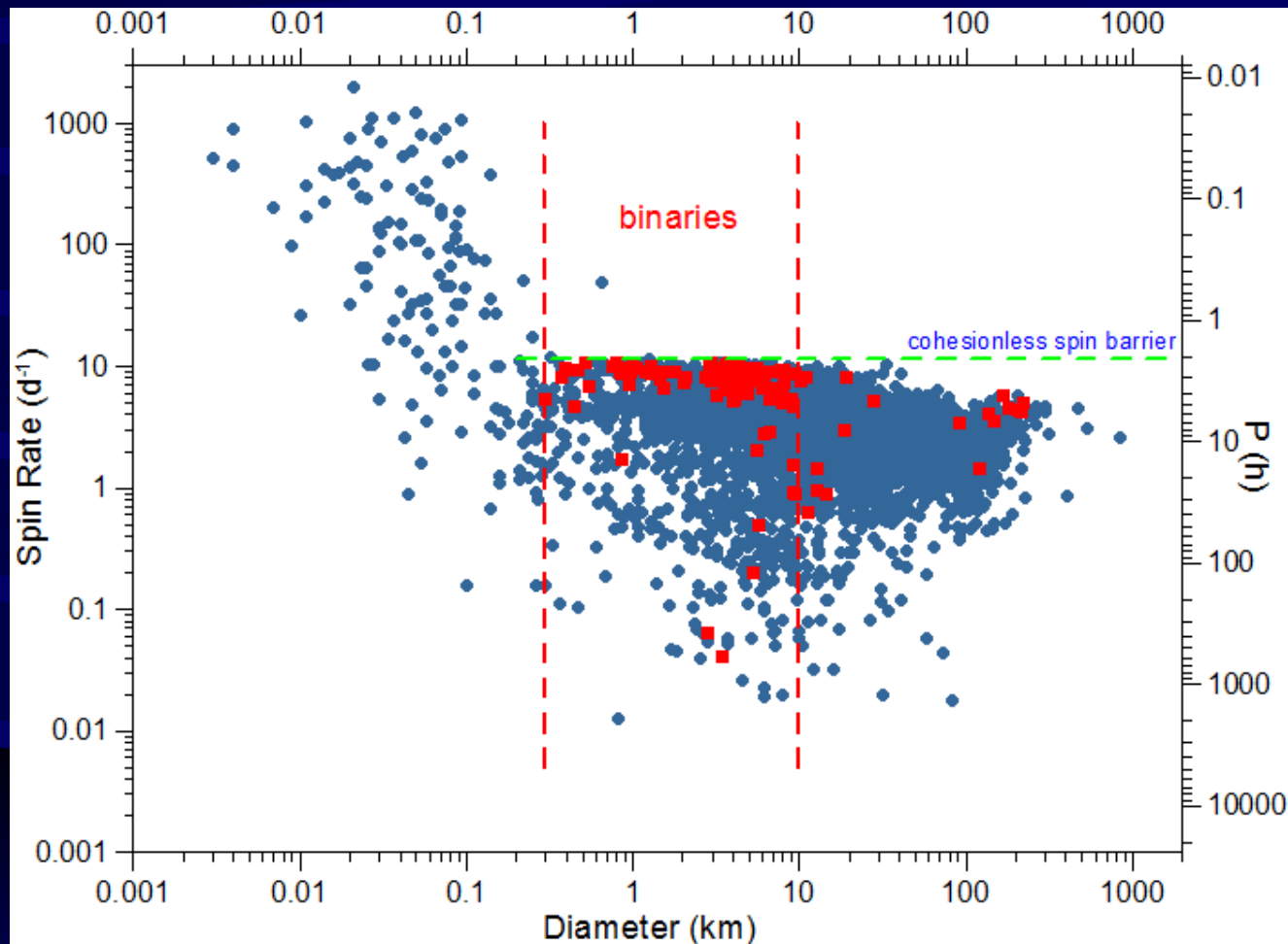
Numerous indirect evidence for that km-sized asteroids are

- predominantly cohesionless structures, with zero global tensile strength.

Some of the most important observations:

- “Spin barrier” – km-sized asteroids rotate slower than the critical rotation frequency for a body in the gravity regime, they can be held together by self-gravitation only.
- Properties of small binary systems and asteroid pairs – dominant formation mechanism is a rotational fission at the cohesionless spin barrier.

The spin barrier

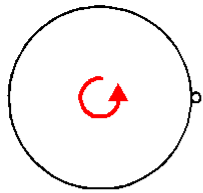


At the spin barrier – balance between the gravity and centrifugal acceleration at the equator of a sphere with $\rho \sim 3 \text{ g/cm}^3$, taking into account also the angle of friction (30-40°).

where $\omega_{csp h}$ is the critical spin rate for the sphere

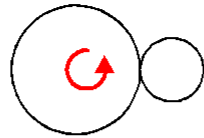
$$\omega_{csp h} = \sqrt{\frac{4}{3}\pi\rho G},$$

The spin barrier in 2nd dimension



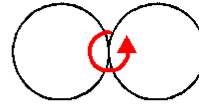
$$R_2 \ll R_1$$

$$\omega_c = \sqrt{\frac{4\pi\rho G}{3}}$$



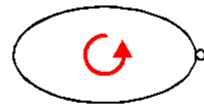
$$X \equiv \frac{R_2}{R_1}$$

$$\omega_c = \sqrt{\frac{4\pi\rho G}{3}} \sqrt{\frac{1}{(1+X)^3(1-\frac{1}{1+X^3})}}$$



$$R_2 = R_1$$

$$\omega_c = \sqrt{\frac{\pi\rho G}{3}}$$



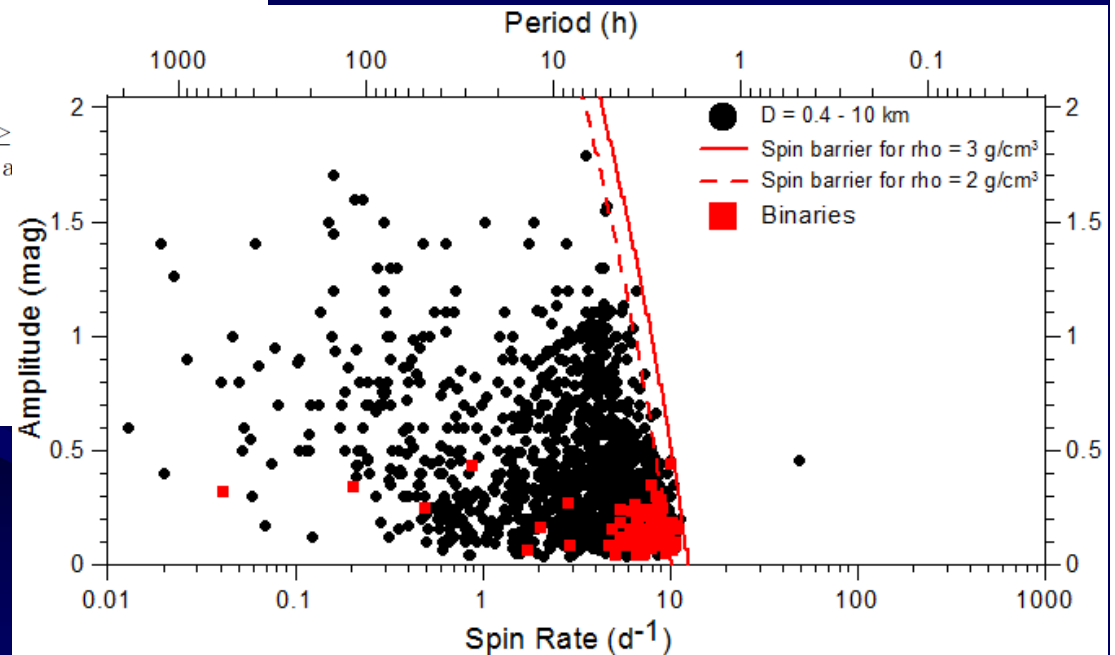
The critical spin rate $\omega_c(90^\circ)$ for a prolate spheroid ($a \geq$ of friction $\phi = 90^\circ$) has been derived by Richardson et al formula

$$\omega_c(90^\circ) = \frac{\sqrt{2\pi\rho G}}{w^{3/2}} \sqrt{(w^2 - 1) \left[2w + \ln \left(\frac{1-w}{1+w} \right) \right]},$$

where $w \equiv \sqrt{1 - (b/a)^2}$.

Spin barrier in 2nd dimension (asteroid elongation).

Vast majority of asteroids larger than ~0.3 km rotate slower than the critical rate for bulk density 3 g/cm³.



Accounting for angles of friction $< 90^\circ$ with theory of cohesionless elastic-plastic solid bodies (Holsapple 2001, 2004).

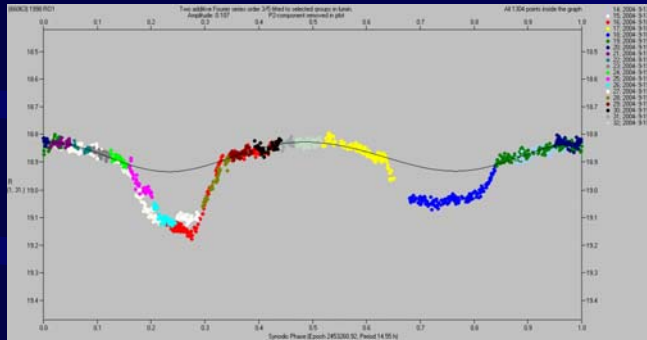
Binary systems among NEAs and small MBAs

Observations

Binary asteroids detection techniques

NEA binaries

- **photometric technique** – detection of mutual events (17 since 1997)
- **radar** – currently the best technique for NEA binaries (24 since 2000)



MBA binaries ($D_1 < 10$ km)

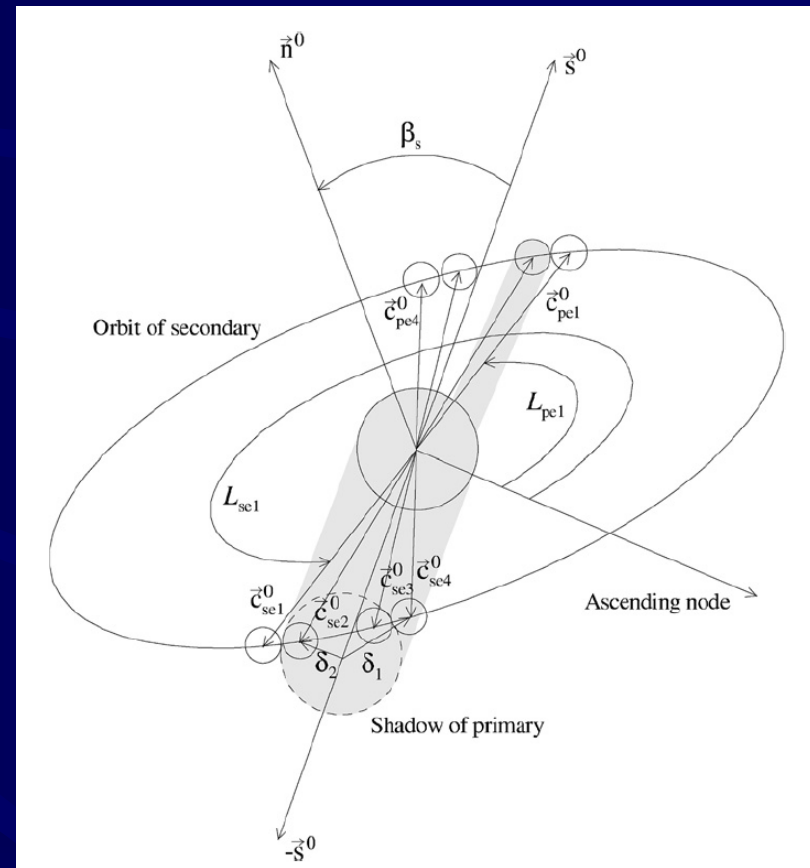
- **photometric technique** – efficient for close systems that appear to predominate in the binary population (59 since 2004).
- **AO observations** – resolve distant satellites (5 since 2002).

Photometric detection of binary system - principle

Mutual occultation/eclipse events
between system components cause
brightness attenuations.

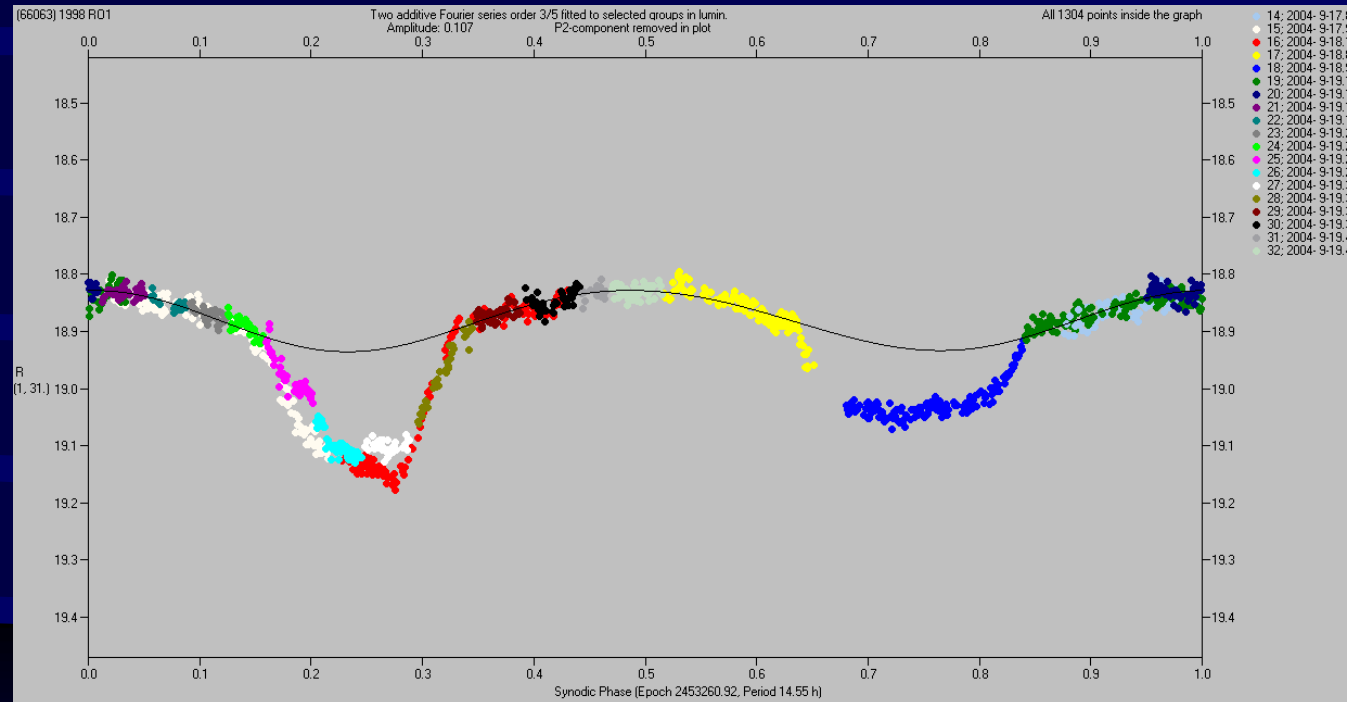
Condition:
Earth or Sun close to the system's orbit
plane.

Primary and secondary events
(depending on which body is
occulted/eclipsed).

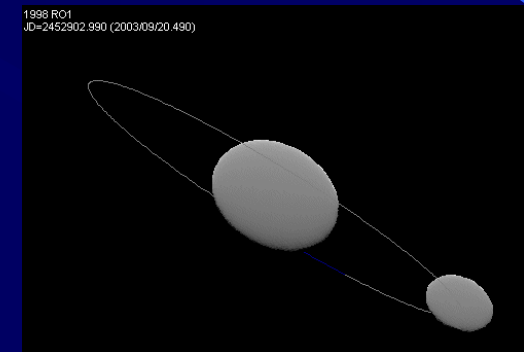


(Scheirich and Pravec 2009)

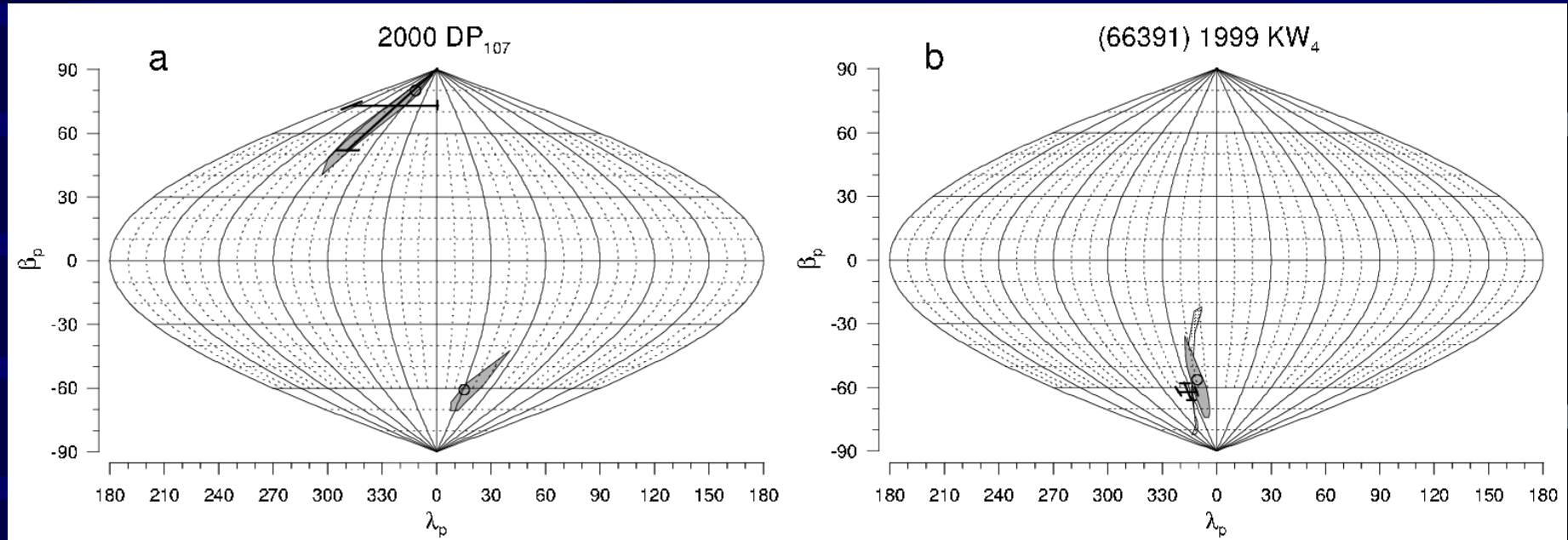
Photometric detection of binary system - example



Derivable parameters: P_1 , P_{orb} , (P_2) , D_2/D_1 , a_1/b_1 , (a_2/b_2)
and finally (with long-arc observations) L_p , B_p , e



Orbit poles – few data so far



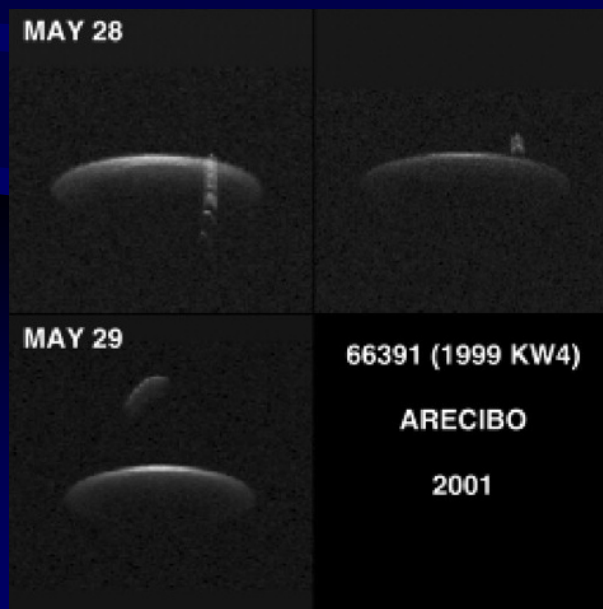
Good data covering long enough “arc” (range of geometries) for a few binaries only (*Scheirich and Pravec 2009*)

Observations of binaries in their return apparitions needed to constrain orbit pole distribution.

Unique radar case – 1999 KW4

The best characterized binary: (66391) 1999 KW4 observed with the Arecibo radar in 2001. The detailed model constructed by *Ostro et al. (Science 314, 1276-1280, 2006)* and the dynamical configuration studied by *Scheeres et al. (Science 314, 1280-1283, 2006)*.

This binary's characteristics appear to be rather typical for NEA binary systems.



Binary asteroid parameters database

Asteroid Spin Statistics

Show View Find Compute Export

Values Uncert's Methods Ref's

List Locked for editing

Object	D1(km)	D2/D1	D2(km)	H	pv	P1(h)	Porb(h)	P2(h)	A1	A2	SoIph	a/b_1	b/c_1	a/b_2	b/c_2	A(km)	A/D_1	rho_1	Peqsph	alpha_1	log(Tt_orb)	log(Tt_1)
(1338) Duponta	8	0.23	1.9	12.84	(0.18)	3.85453	17.57	(17.57)	0.26	0.04	20	1.20		1.7		(16)	(2.0)	(2.0)	3.13	0.75	8.2	
(1509) Escalangona	7.8	0.33	2.6		0.23	3.247	(874)		0.13		26	1.09				(210)	(27)	(2.0)	(1.65)	(1.41)	(15.2)	(
(1717) Arion	9	(0.6)	(6)	12.3	(0.18)	(5.148)	117.0	(18.23)	(0.08)	(0.13)	11	(1.09)		(1.5)		(70)	(7.5)	(2.0)	(1.28)	(1.82)	(10.6)	(
(1830) Pogson	9	(0.4)	(4)	(12.45)	(0.18)	2.5702	24.240		0.12		5	1.12				(23)	(2.5)	(2.0)	(1.88)	(1.24)	(8.0)	
(1862) Apollo	1.7	0.04	0.075	16.23	0.20	3.0662						1.27						(2.0)				
(2006) Polonskaya	6.4	(0.23)	(1.5)	13.4	(0.18)	(3.1179)	19.15		(0.08)		11	(1.07)				(13)	(2.1)	(2.0)	(0.87)		(8.6)	
(2044) Wirt	7	0.25	1.7	13.3	(0.18)	3.6897	18.97	(18.97)	0.26	(0.035)	20	1.20		(1.5)		(14)	(2.1)	(2.0)	2.95	0.79	8.4	
(2478) Tokai	8	0.86	7	12.33	(0.18)	25.891	25.891	25.891	(0.20)	(0.20)	9	(1.31)		(1.4)		(25)	(3.0)	(2.0)	1.67	1.40	7.6	
(2486) Metsahovi	8	(0.7)	(5)	12.59	(0.18)	(2.6404)		(4.4518)	0.04	0.12	12	1.05		1.3								
(2754) Efimov	6	0.20	1.2	(13.5)	(0.18)	2.4497	14.765		0.15		18	1.11				(11)	(1.8)	(2.0)	2.16	1.08	8.3	
(3073) Kursk	5.5	0.25	1.4	13.73	(0.18)	3.4468	44.96		0.21		15	1.17				(20)	(3.7)	(2.0)	2.71	0.86	10.2	
(3309) BrorFelde	5.0	0.26	1.3	13.9	(0.18)	2.5041	18.48	18.47	0.09	0.04	9	1.08		1.7		(10)	(2.0)	(2.0)	2.15	1.09	8.6	
(3671) Dionysus	1.5	0.2	0.3	16.67	0.16	2.7053	27.74		0.12	(0.03)	30	1.07		(1.6)		(4.0)	(2.7)	(2.0)	2.38	0.98	10.7	
(3703) Volkonskaya	2.7	0.4	1.1	(14.3)	(0.4)	3.235	(24)		0.22		6	1.23				(6.7)	(2.5)	(2.0)	(2.15)	(1.09)	(9.1)	
(3749) Balan	6	0.22	1.4	(13.4)	(0.18)		2640									310	(56)	(2.0)			17.9	
(3782) Celle	6	0.43	2.6	(12.5)	(0.4)	3.839	36.57		0.12		7	1.12				(20)	(3.3)	(2.0)	2.21	1.06	9.1	
(3982) Kastei	5.2	(0.8)	(4.2)	13.35	(0.18)	(5.8358)		(8.4865)	(0.08)	(0.26)	7	(1.11)		(1.7)				(2.0)				
(4029) Bridges	8	0.24	1.9	(12.9)	(0.18)	3.5746	16.31		0.20		2	1.21				(15)	(1.9)	(2.0)	2.90	0.81	8.0	
(4492) Debussy	11	0.93	10	(12.9)	(0.058)	(26.606)	26.606	(26.606)	(0.2)	(0.2)	12	(1.32)		(1.4)		(34)	(3.2)	(2.0)	1.60	1.46	7.4	
(4674) Pauling	3.7	0.32	1.2	14.0	(0.3)	2.5306	(3550)		0.06		16	1.05				(250)	(68)	(2.0)	(1.21)	(1.93)	(18.5)	(
(4786) Tatiana	7	0.19	1.3	(13.2)	(0.18)	2.9227	21.67		0.20		10	1.17				(16)	(2.3)	(2.0)	2.49	0.94	9.0	
(4951) Iwamoto	4.0	0.88	3.5	13.74	(0.20)	118.0	118.0	118.0	(0.17)	(0.17)	14	(1.24)		(1.3)		(33)	(8.4)	(2.0)	1.04	2.25	11.1	
(5381) Sekhmet	1.0	0.30	0.3	(16.5)		2.7	12.5	10	(0.1)		65					1.54	1.54	1.8	2.27	1.07	9.1	
(5407) 1992 AX	3.9	(0.2)	(0.8)	14.47	(0.18)	(2.5488)	(13.520)		(0.10)		7	(1.09)				(6.5)	(1.7)	(2.0)	(2.26)	(1.08)	(8.5)	
(5477) 1989 UH2	3.0	0.37	1.1	14.4	(0.3)	2.9941	24.42		0.11		3	1.11				(7.5)	(2.5)	(2.0)	2.18	1.07	9.1	
(5905) Johnson	3.6	0.38	1.4	14.0	(0.3)	3.7824	21.785		0.10		20	1.08				(8.3)	(2.3)	(2.0)	2.59	0.90	8.7	
(6084) Bascom	7	0.37	2.5	13.2	(0.18)	2.7454	43.5	43.5	0.22	0.04	10	1.21		1.3		(25)	(3.7)	(2.0)	1.90	1.23	9.5	
(6244) Okamoto	5.1	0.25	1.3	13.86	(0.18)	2.8958	20.32		0.11		8	1.10				(11)	(2.2)	(2.0)	2.45	0.95	8.8	
(7088) Ishtar	1.2	0.42	0.5	16.9	(0.18)	2.6787	20.63	20.60	0.11	0.10	21	1.09		1.6		(2.7)	(2.2)	(2.0)	1.93	1.21	9.4	
(9069) Howland	3.0	(0.4)	(1.2)	(14.4)	(0.3)	(4.2175)	(30.33)	(30.33)	(0.09)	(0.09)	18	(1.07)		(1.6)		(9)	(2.9)	(2.0)	(2.55)	(0.91)	(9.4)	
(9260) Edwardolson	3.8	0.27	1.0	14.5	(0.18)	3.0854	17.785		0.11	(0.04)	7	1.10		(1.6)		(8)	(2.0)	(2.0)	2.56	0.91	8.7	
(9617) Grahanchapman	5	0.27	1.2	(14.1)	(0.18)	2.2856	19.385		0.10		8	1.09				(10)	(2.1)	(2.0)	1.96	1.19	8.7	
(11264) Claudionaccone	4.2	0.4	1.7	14.20	(0.18)	3.1872	15.11		0.12		10	1.11				(8)	(1.8)	(2.0)	2.29	1.02	7.8	
(17246) 2000 GL74	4.2	0.40	1.7	(14.0)	(0.22)		2034									228	(48)	(2.0)			17.1	
(17260) 2000 JQ58	5	0.26	1.2	(14.0)	(0.18)	3.1287	14.757	14.75	0.15	0.07	10	1.13		2.5		(8)	(1.8)	(2.0)	2.60	0.90	8.2	
(22899) 1999 T014	4.3	0.32	1.4	(14.0)	(0.22)		1356									182	(36)	(2.0)			16.5	
(31345) 1998 PG	0.9	(0.4)	(0.34)	17.64	(0.18)	(2.5162)	(14.01)	(14.01)	(0.11)	(0.09)	22	(1.09)		(1.5)		(1.5)	(1.7)	(2.0)	(1.95)	(1.20)	(9.1)	
(34706) 2001 OP83	3.2	0.28	0.9	14.9	(0.18)	2.5944	20.76		0.13		11	1.11				(7.0)	(2.2)	(2.0)	2.16	1.08	9.1	
(35107) 1991 UH	1.2	0.38	0.45	16.98	(0.18)	2.6237	32.67	(12.836)	0.08	(0.06)	27	1.06		(1.3)		(3.6)	(3.0)	(2.0)	1.93	1.21	10.4	
(65803) Didymos	0.75	0.22	0.17	18.16	0.16	2.2593	11.91	(11.91)	0.08	0.025	8	1.07		1.5		(1.14)	(1.5)	(2.0)	2.02	1.16	9.6	
(66063) 1998 R01	0.8	0.48	0.38	18.04	0.14	2.4924	14.54	14.52	0.13	0.10	11	1.13		1.5		(1.4)	(1.8)	(2.0)	1.77	1.32	9.0	
(66391) 1999 KW4	1.282	0.330	0.423			2.7645	17.422	(17.422)				1.041	1.150	1.322	1.312	2.548	1.99	2.0	2.20	1.06	9.4	
(69230) Hermes	0.6	0.9	0.54	17.57	0.25	(13.894)	13.894	(13.894)	(0.03)	(0.03)	7	(1.04)		(1.06)		(1.2)	(2.0)	(2.0)	1.91	1.22	8.7	
(76818) 2000 RG79	2.8	0.35	0.98	14.26	(0.4)	3.1665	14.127	14.127	0.14	0.06	16	1.12		1.5		(4.8)	(1.7)	(2.0)	2.43	0.96	8.2	
(85938) 1999 DJ4	0.35	0.5	0.17	18.59	0.42	2.5141	17.73	(17.73)	0.11	0.17	63	1.06		1.4		(0.7)	(2.1)	(2.0)	1.73	1.35	10.0	
(88710) 2001 SL9	0.8	0.28	0.22	18.03	(0.16)	2.4004	16.40		0.08		5	1.07				(1.5)	(1.9)	(2.0)	2.06	1.14	9.9	
(114319) 2002 XD58	1.9	(0.5)	(1.0)	15.8	(0.18)	(2.9649)		(7.954)	(0.14)	(0.09)	17	(1.13)		(1.4)				(2.0)				
(137170) 1999 HF1	3.5	0.23	0.8	(14.6)	(0.2)	2.31927	14.03	(14.03)	0.17	0.03	63	1.08		1.3		(6)	(1.7)	(2.0)	2.05	1.14	8.5	
1000 ns	0.3	0.15	0.045	(10.3)			21									(0.7)	(2.2)	(2.0)			12.0	

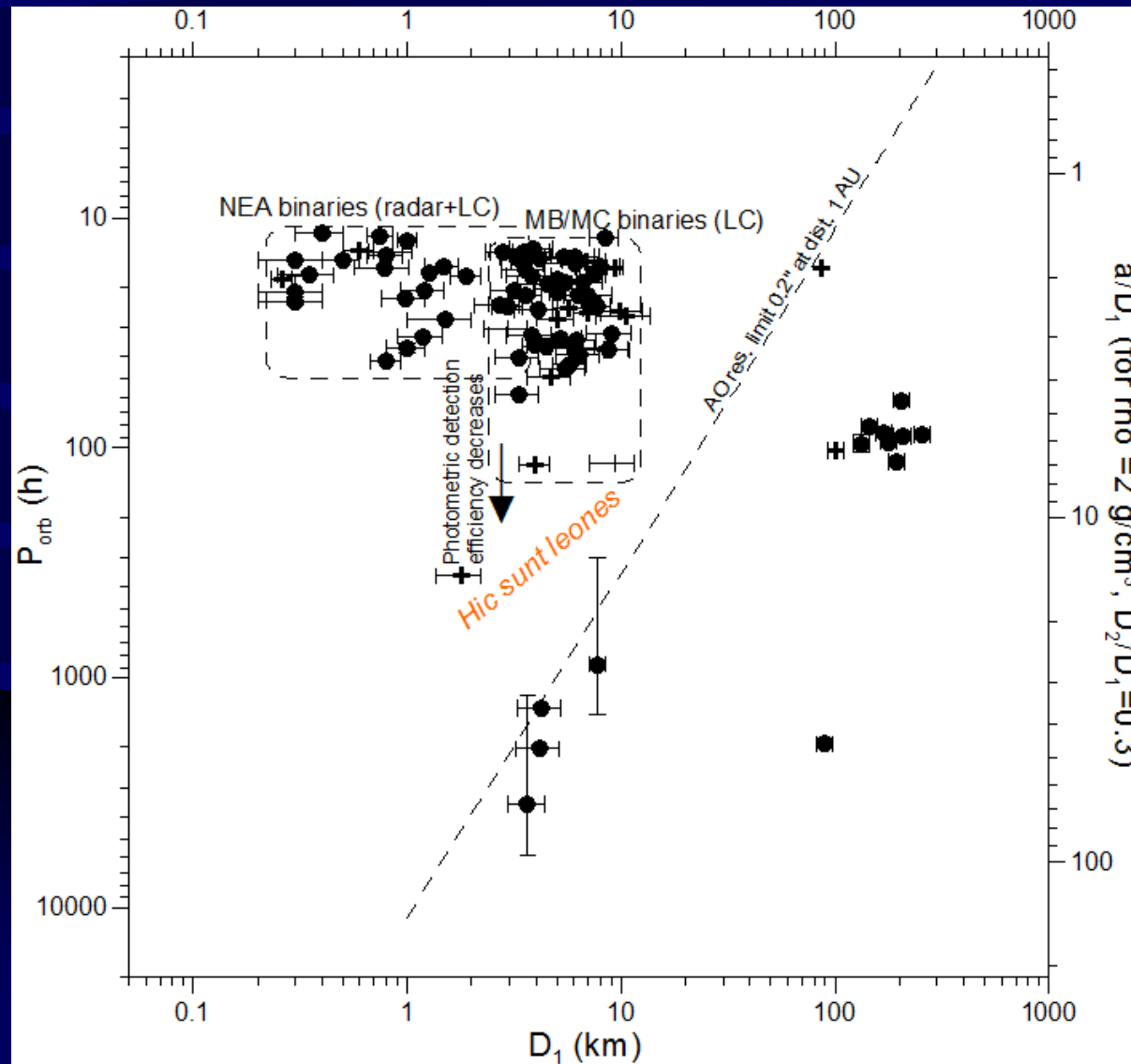
Start | Total Commander 6.53 - ... | Grapher - [fd_pom3.grf] | Microsoft PowerPoint - [c...] | spinst | 10:57

(Pravec and Harris 2007, updated)

Binary systems among NEAs and small MBAs

The population and properties

Binary population P_{orb} vs D_1



Binary fraction
 $15 \pm 4\%$
 among NEAs
 (Pravec et al.
 2006).

Similar binary
 fraction among
 MBAs (up to $D_1 =$
 10 km)

Data from
 Pravec and Harris,
Icarus, 190 (2007)
 250-253, updated.

Characteristic properties of NEA and small MBA binaries

Most NEA and small MBA binaries have common characteristics:

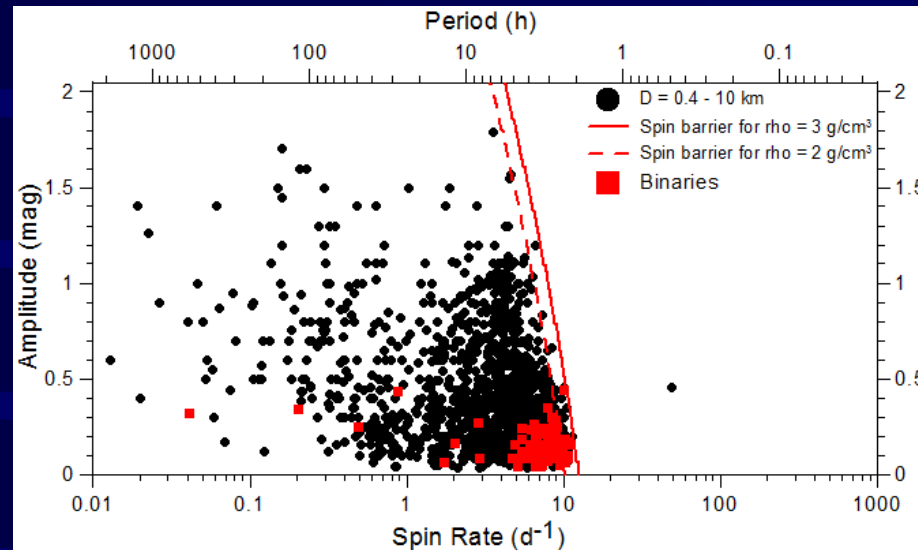
1. Total angular momentum close to critical
2. Primaries – near spheroidal shapes (unless in rare cases of fully synchronous systems)
3. Secondaries - a broader distribution of shape elongations. Rotations mostly, but not always synchronous.

Exceptional systems:

- Double ($D_2/D_1 = 0.8 - 1$), fully synchronous system: 1 case among NEAs so far: Hermes (*Margot et al. 2006*), a few among MBAs
- Ternary systems - two small satellites orbiting a larger primary: 2 cases among NEAs so far, (136617) 1994 CC and (153591) 2001 SN263 (*Nolan et al. 2008, Brozovic et al. 2009*)
- “Quadruple” system (3749) Balam – One close and one distant satellite, plus a paired asteroid 2009 BR60 (*Merline et al. 2002, Marchis et al. 2008, Vokrouhlický et al. 2009*)

Characteristic properties of binaries

1. Angular momentum content



Primary rotations

- concentrate in the pile up at $f = 6-11 \text{ d}^{-1}$ ($P_1 = 2-4 \text{ h}$) in front of the spin barrier.

A tail with slowed down primaries – members of systems with high D_2/D_1 where a large part of the system's angular momentum resides in the orbital motion and secondary's rotation.

Total angular momentum similar, and close to critical in all binaries with $D_1 < 10$ km.

Characteristic properties of binaries

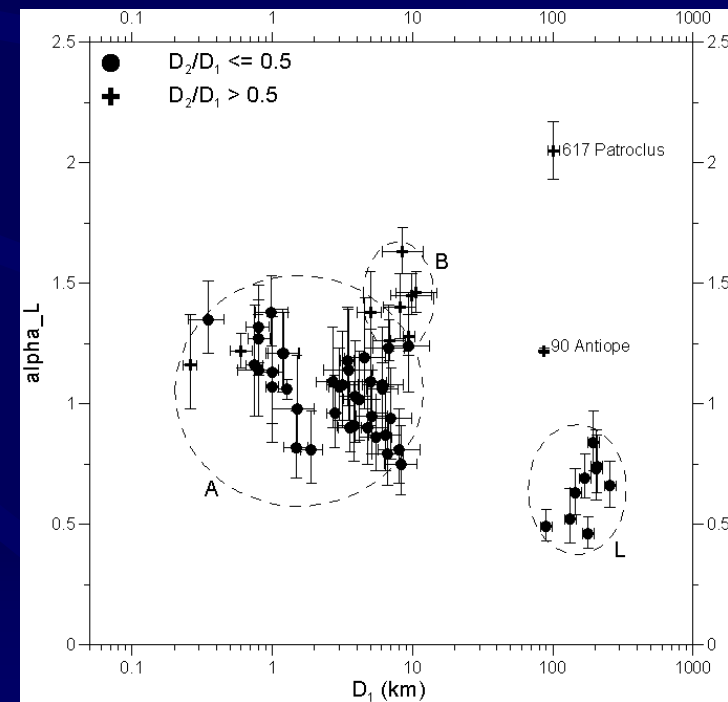
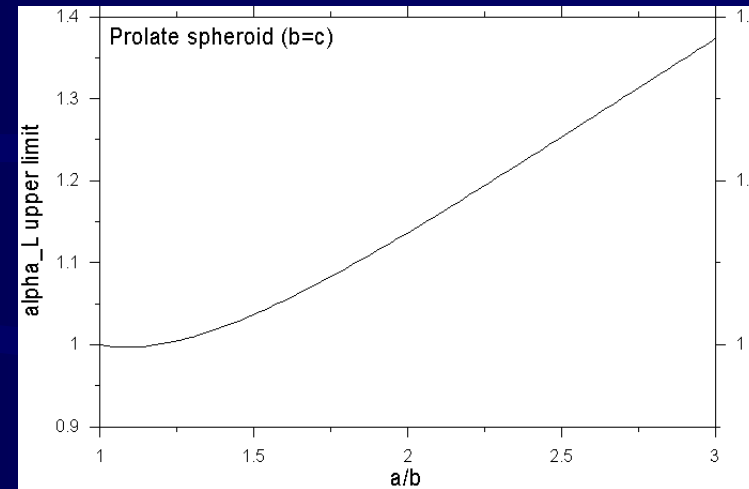
1. Angular momentum content

$$\alpha_L = L_{tot}/L_{critsph}$$

where L_{tot} is a total angular momentum of the system, $L_{critsph}$ is angular momentum of an equivalent (i.e., the same total mass and volume), critically spinning sphere.

Binaries with $D_1 \leq 10$ km have α_L between 0.9 and 1.3, as expected for systems originating from critically spinning rubble piles.

(Pravec and Harris 2007)



Characteristic properties of binaries

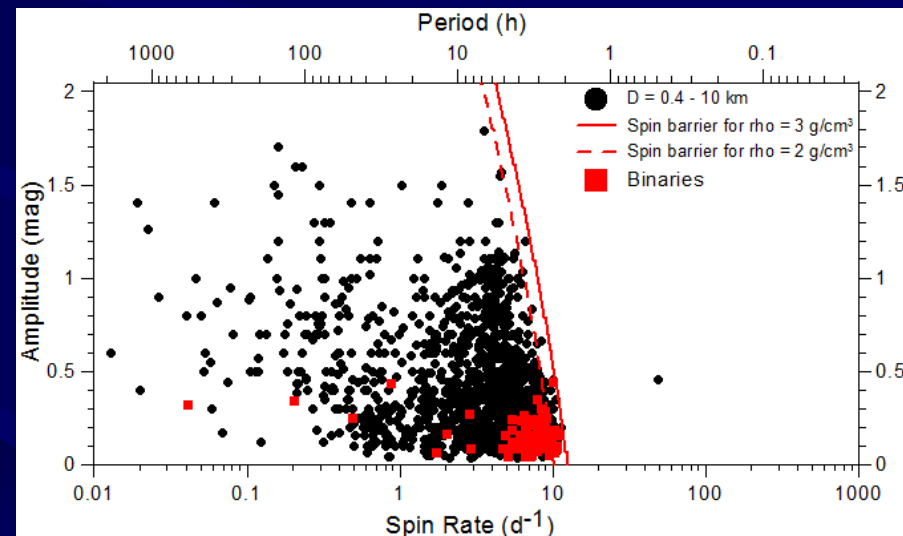
2. Primary shapes

Primaries of asynchronous binaries:

- spheroidal, low equatorial elongations, $a/b = 1.1 \pm 0.1$ for $> 90\%$ of systems

A primary shape not far from rotational symmetry seems to be a requirement for satellite formation or orbital stability (*Walsh et al. 2008, Scheeres 2007*).

Model of the primary of 1999 KW4 (*Ostro et al. 2006*)



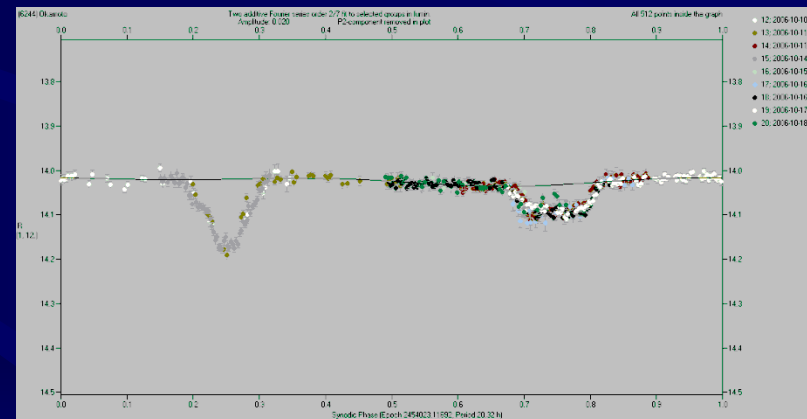
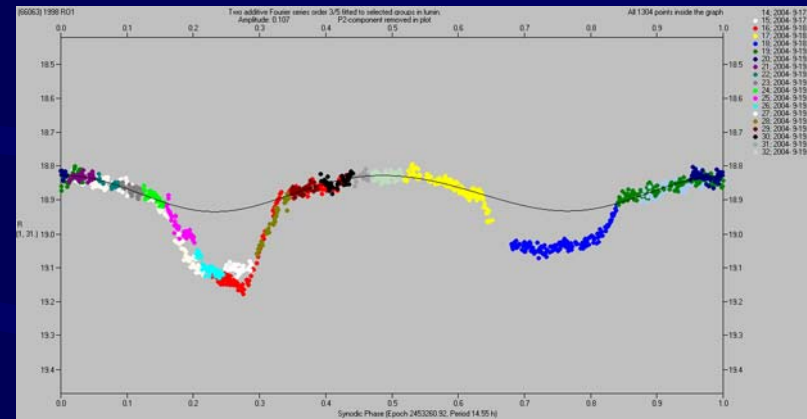
Characteristic properties of binaries

3. Secondary shapes and rotations

Broader range of equatorial elongations: $a/b = 1:1$ to $2:1$.

Mostly synchronous rotation, but some not.

Interpretation of a third period (P_{orb} , P_1 , P_2) often ambiguous though – may be an unsynchronous rotation of the secondary, or a rotation of a third body.



Binary formation theories

Ejecta from large asteroidal impacts (e.g., *Durda et al. 2004*) – does not predict the observed critical spin.

Tidal disruptions during close encounters with terrestrial planets (*Bottke et al. 1996; Richardson and Walsh*) – does not work in the main belt, so, it cannot be a formation mechanism for MB binaries. It may contribute to and shape the population of NEA binaries.

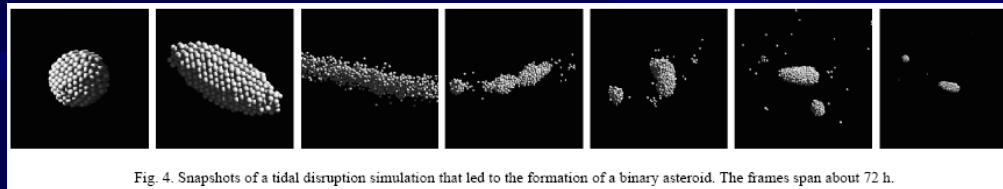


Fig. 4. Snapshots of a tidal disruption simulation that led to the formation of a binary asteroid. The frames span about 72 h.

(*Walsh and Richardson 2006*)

Fission of critically spinning parent bodies spun up by YORP (e.g., *Walsh et al. 2008*) – appears to be a primary formation mechanism for small close binaries.

Asteroid pairs among small MBAs

Related to orbiting (bound) binaries –
formation by rotational fission

Asteroid Itokawa

Can it fission when spun up?

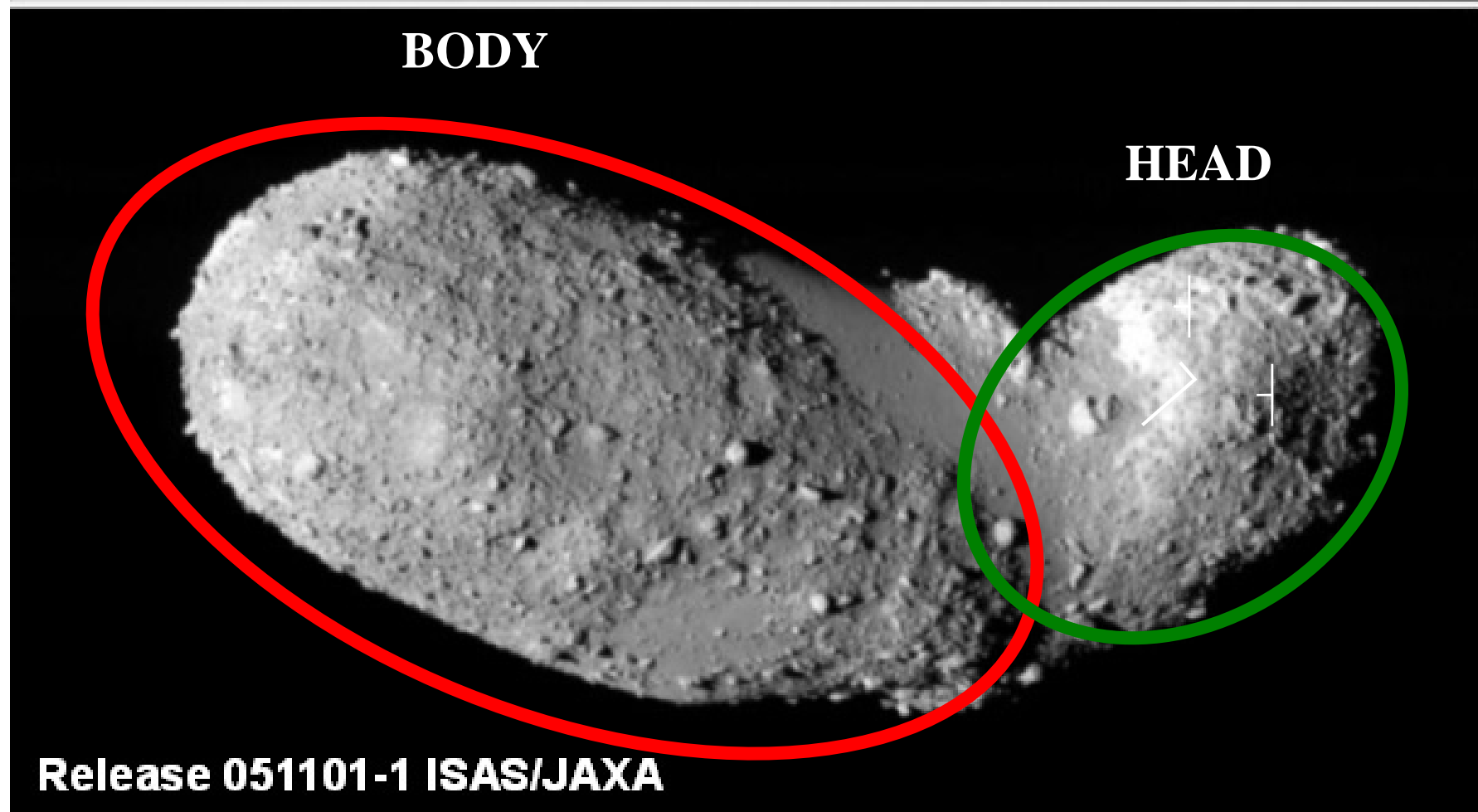


図3 イトカワの +90 度面

Asteroid pairs

found on closely similar heliocentric orbits

Vokrouhlický and Nesvorný (Astron. J. 136, 280, 2008; VN08) found a population of pairs of asteroids residing on closely similar orbits.

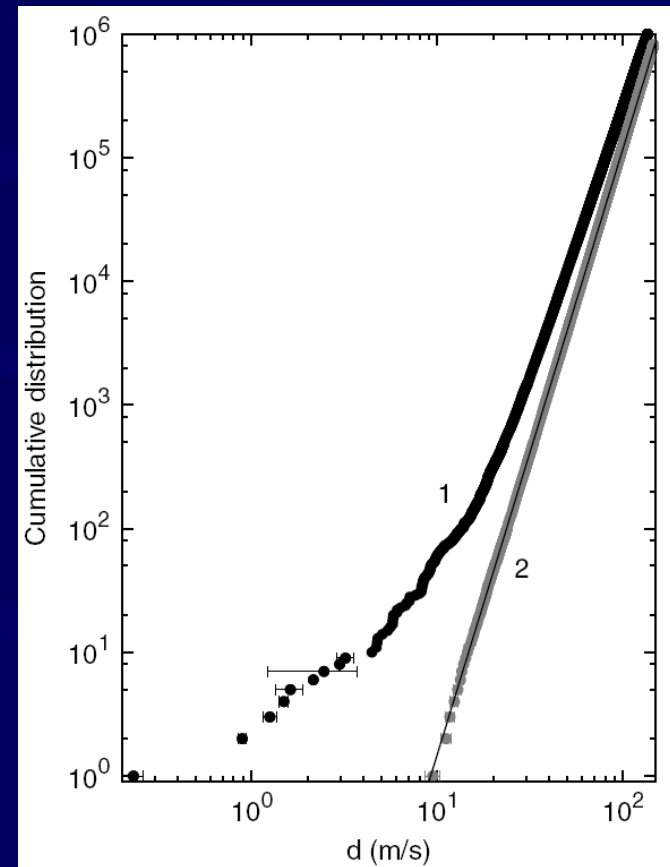
Pravec and Vokrouhlický (Icarus 204, 580, 2009; PV09) extended the analysis and found numerous significant pairs up to $d = 36$ m/s (approx. the current relative encounter velocity between orbits).

d in 5-dimensional space of osculating orbital elements $(a, e, i, \varpi, \Omega)$ defined as a positive-definite quadratic form:

$$\left(\frac{d}{na}\right)^2 = k_a \left(\frac{\delta a}{a}\right)^2 + k_e (\delta e)^2 + k_i (\delta \sin i)^2 + k_\Omega (\delta \Omega)^2 + k_\varpi (\delta \varpi)^2, \quad (1)$$

where n and a is the mean motion and semimajor axis of either of the two asteroids and $(\delta a, \delta e, \delta \sin i, \delta \varpi, \delta \Omega)$ is the separation vector of their orbital elements.¹

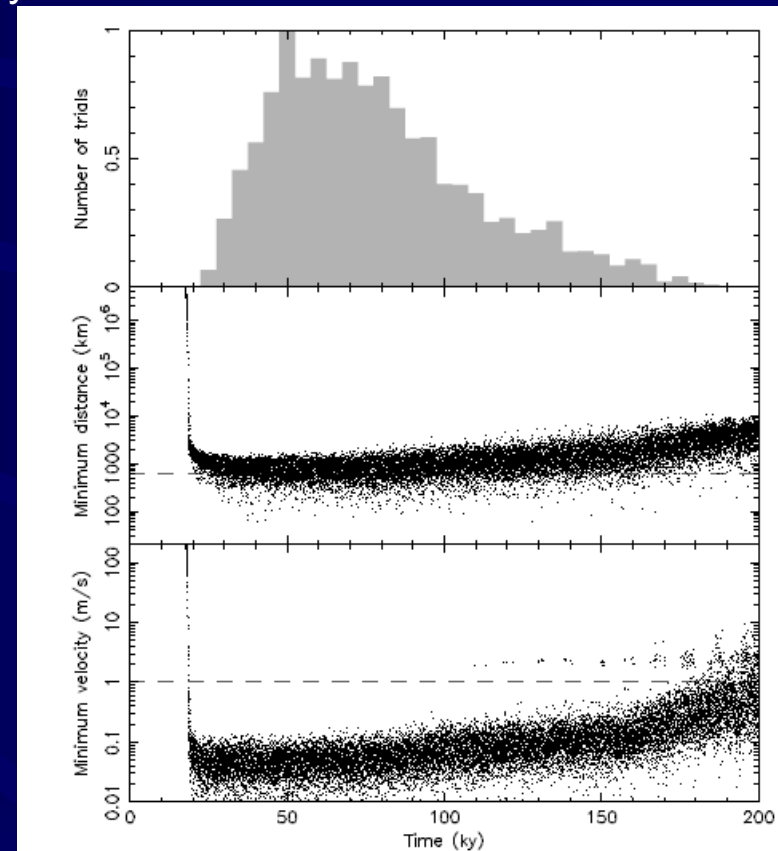
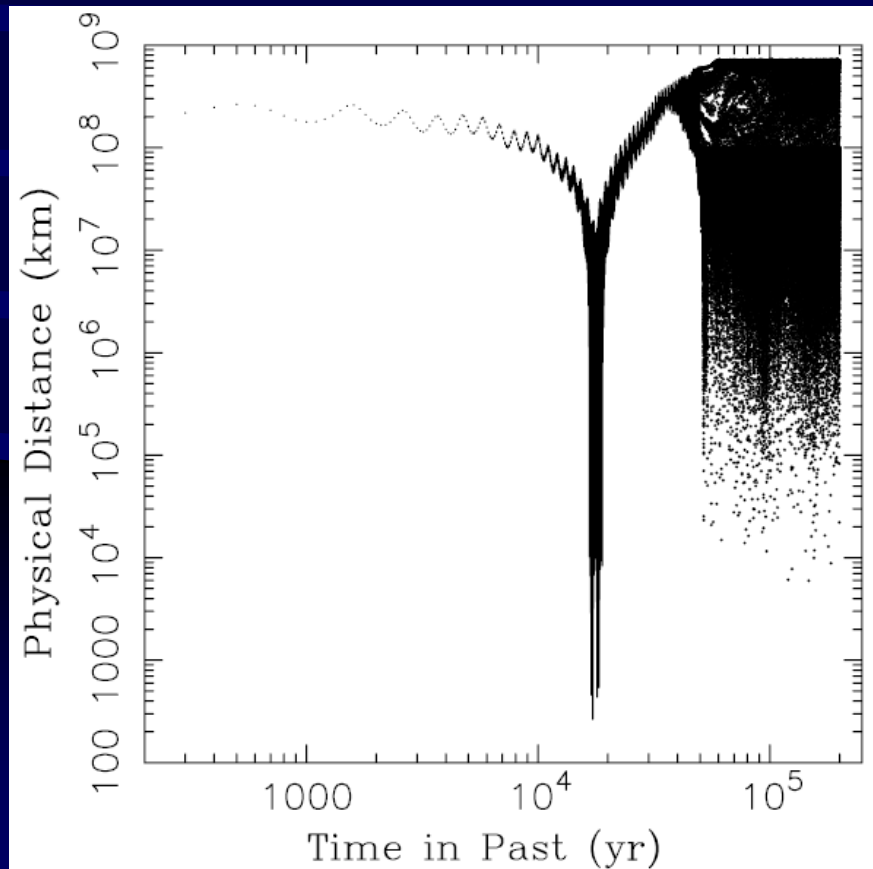
	a	e	i	Omega	omega
4765	1.9455258	0.0604289	23.70505	76.59085	108.05341
2001X0105	1.9455837	0.0604382	23.70634	76.52980	108.30700
	-0.0000578	-0.0000093	-0.00129	0.06105	-0.25359



Asteroid pairs

identification method by Pravec and Vokrouhlický (2009)

Candidate pairs identified by computing probabilities of chance coincidence of unrelated asteroids from the background population. Pairs with probabilities $p2/Np < 1\%$ are secure (confirmed with backward orbit integrations), while pairs with higher probabilities of being chance coincidences are checked more thoroughly.



Supplementary Figure 2: Results of the backward integration of 2500 geometric and Yarkovsky clones for each of the components in the pair (21436) Chaoyichi and 2003 YK39. At each

Origin of asteroid pairs - proposed theories

VN08 proposed a number of possible origins for these asteroid pairs:

Formation in catastrophic impact disruptions

- *No a priori bounds on spin rates of resulted bodies predicted*

Formation by rotational fission due to YORP spin-up

- a. A cohesive body spun beyond its fission limit could break and immediately send off its components on escape orbits

PREDICTION: *Both components spin rapidly, no a priori bounds on mass ratio*

- b. A “cohesionless” (“rubble pile”) body could spin fission, form a proto-binary asteroid, and then subsequently escape

PREDICTION (Scheeres 2007, 2009): *Mass ratios should be less than ~ 0.2 , primaries of higher mass ratio systems should have longer rotation periods, primaries of lower mass ratio systems should spin closer to surface disruption spin limits*

Disruption of an existing binary

- Expansion of a binary due to BYORP or other effect could cause a binary system to mutually escape

PREDICTION: *Mass ratios should mimic binary population, secondaries may be slow rotating, primary spin periods should mimic binary population*

Origin of asteroid pairs - proposed theories

VN08 proposed a number of possible origins for these asteroid pairs:

Formation in catastrophic impact disruptions

- *No a priori bounds on spin rates of resulted bodies predicted*

Formation by rotational fission due to YORP spin-up

- a. A cohesive body spun beyond its fission limit could break and immediately send off its components on escape orbits

PREDICTION: *Both components spin rapidly, no a priori bounds on mass ratio*

- b. A “cohesionless” (“rubble pile”) body could spin fission, form a proto-binary asteroid, and then subsequently escape (Pravec et al. 2010)

PREDICTION (Scheeres 2007, 2009): *Mass ratios should be less than ~ 0.2 , primaries of higher mass ratio systems should have longer rotation periods, primaries of lower mass ratio systems should spin closer to surface disruption spin limits*

Disruption of an existing binary

- Expansion of a binary due to BYORP or other effect could cause a binary system to mutually escape

PREDICTION: *Mass ratios should mimic binary population, secondaries may be slow rotating, primary spin periods should mimic binary population*

Pair formation by spin fission due to YORP spin-up

If mass ratio $\lesssim 0.2$

The total angular momentum and energy are, in general, conserved across fission but becomes decomposed into multiple components:

$$\mathbf{I} \cdot \boldsymbol{\omega} = \mathbf{I}_1 \cdot \boldsymbol{\omega}_1 + \mathbf{I}_2 \cdot \boldsymbol{\omega}_2 + \frac{M_1 M_2}{M_1 + M_2} \mathbf{r} \times \mathbf{v} \quad (7)$$

$$\frac{1}{2} \boldsymbol{\omega} \cdot \mathbf{I} \cdot \boldsymbol{\omega} + \mathcal{U} = \frac{1}{2} \boldsymbol{\omega}_1 \cdot \mathbf{I}_1 \cdot \boldsymbol{\omega}_1 + \frac{1}{2} \boldsymbol{\omega}_2 \cdot \mathbf{I}_2 \cdot \boldsymbol{\omega}_2 + \frac{1}{2} \frac{M_1 M_2}{M_1 + M_2} \mathbf{v} \cdot \mathbf{v} + \mathcal{U}_{11} + \mathcal{U}_{22} + \mathcal{U}_{12} \quad (8)$$

where M_1 and M_2 are the masses of the two components, \mathbf{r} and \mathbf{v} are the relative position and velocity vector between these two components, \mathcal{U}_{ii} is the self-potential of the new components and \mathcal{U}_{12} is the mutual potential between the components.

$$\mathcal{U}_{12} = -G \int_{\beta_1} \int_{\beta_2} \frac{dm_1 dm_2}{|\boldsymbol{\rho}_1 - \boldsymbol{\rho}_2|} \quad (9)$$

The mutual potential represents a conduit for energy being transferred from rotational to translational energy and vice-versa and can be surprisingly effective.

Model of the proto-binary separation

- explains the observed correlation P_1 vs q

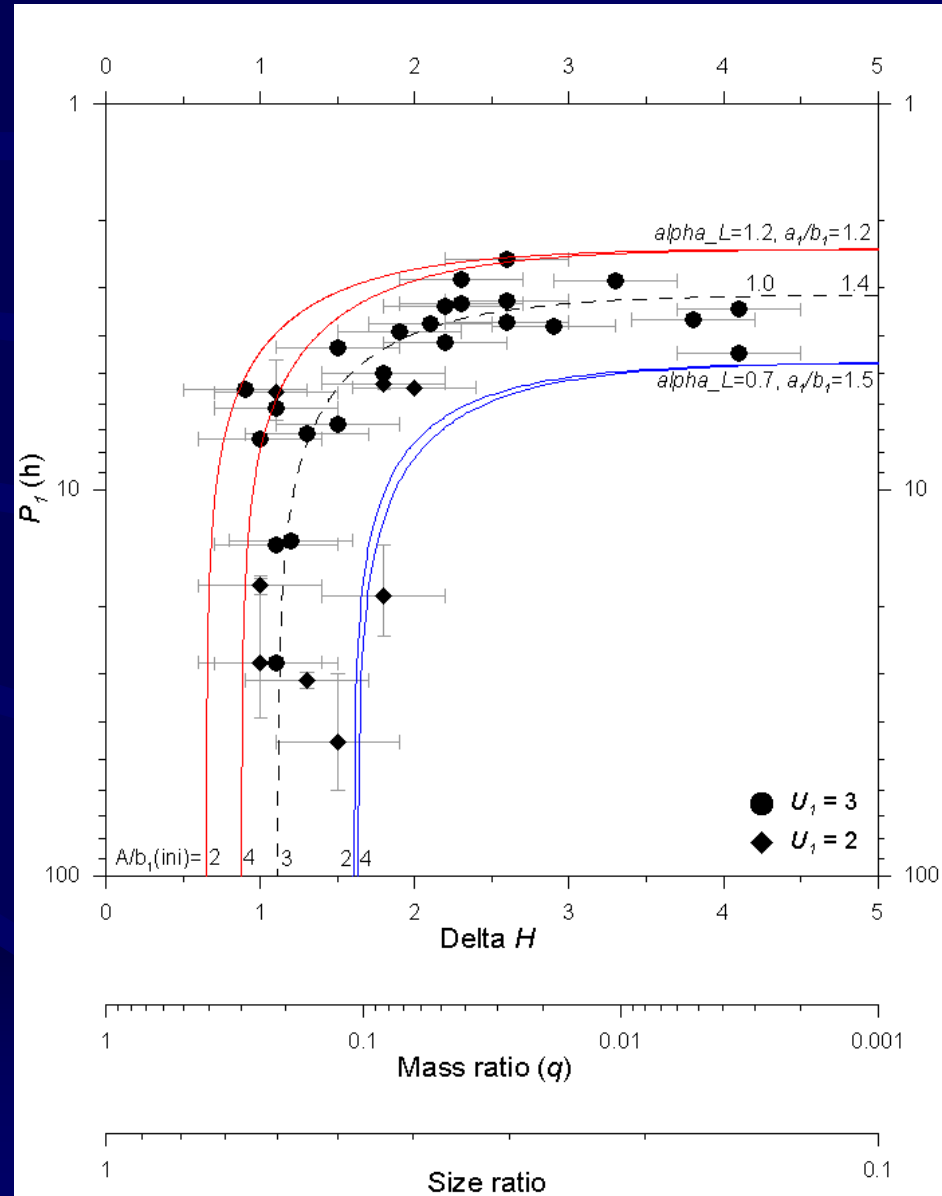
Model curves for following parameters:

- $\alpha_L = 0.7, 1.0, 1.2$
(total angular momentum near the lower, middle and upper values observed in orbiting binary systems)
- initial separations $A/b_1 = 2$ and 4
(orbit's semimajor axis/medium semiaxis of the primary)
- primary's equatorial axes ratio $a_1/b_1 = 1.2 - 1.5$ (from observed amplitudes).

Primaries of pairs with small mass ratios ($q = 10^{-3}$ to a few 10^{-2}) rotate rapidly near the critical fission frequency.

As the mass ratio approaches the approximate cutoff limit of 0.2, the primary period grows long, as when the total energy of the system approaches zero to disrupt the asteroid pair must extract an increasing fraction of the primary's spin energy.

Asteroid pairs were formed by rotational fission of critically spinning parent asteroids. (Pravec et al. 2010)



Astrometric detection of binary asteroids with Photocenter variation

Binary system's photocenter displacement

Photocenter displacement vector:

$$\Delta \mathbf{r} = \mathbf{r}[(1 + q)^{-1} - (1 + S)^{-1}], \quad (1)$$

where \mathbf{r} is a projected radius vector, $q \equiv M_2/M_1$ is the mass ratio, and $S \equiv I_2/I_1$ is the brightness ratio between the components of the binary.

For spherical components with the same albedo and phase effect, it is $q = X^3$ and $S = X^2$ and

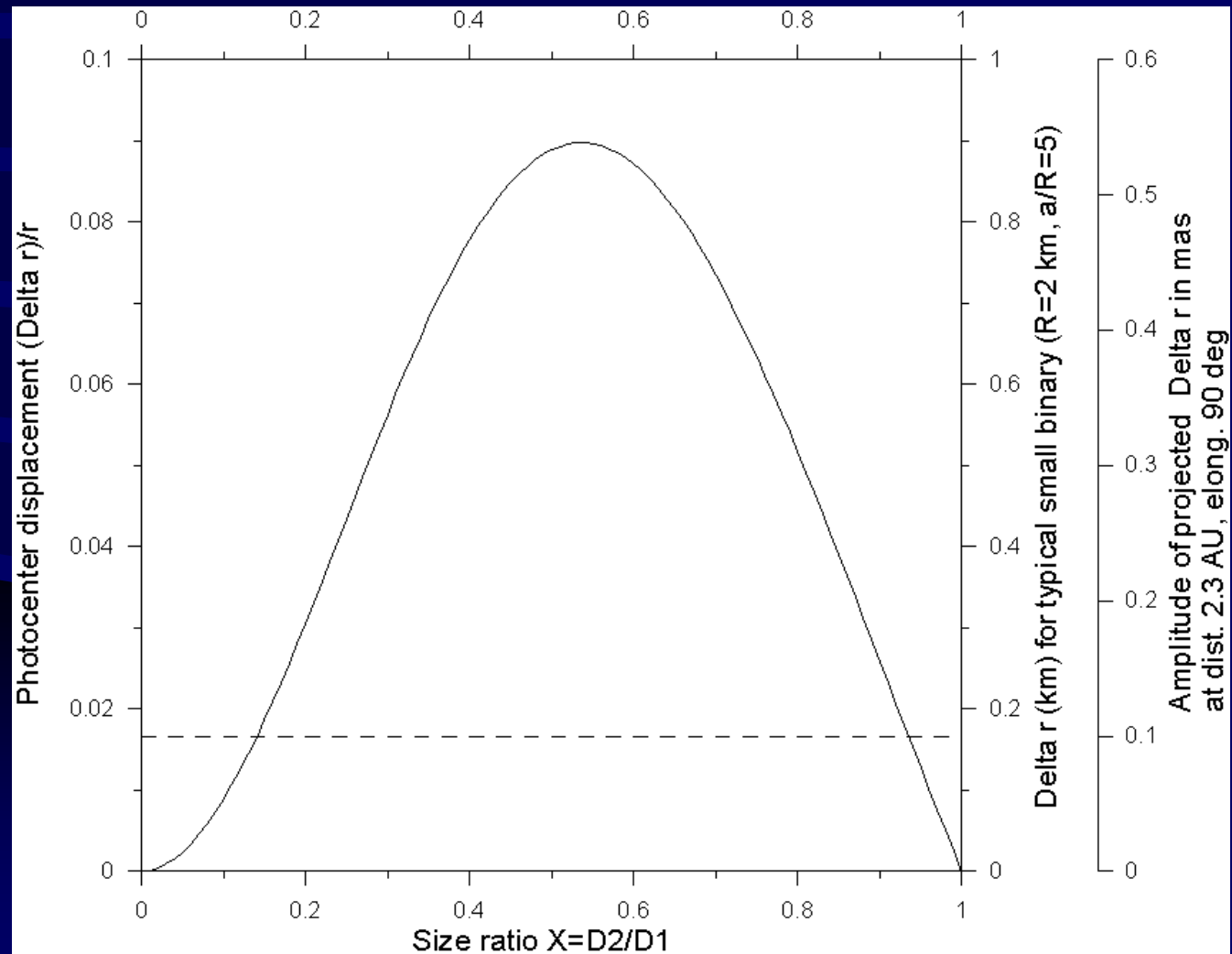
$$\Delta \mathbf{r} = \mathbf{r}[(1 + X^3)^{-1} - (1 + X^2)^{-1}], \quad (2)$$

where $X \equiv D_2/D_1$ is the size ratio between the binary components.

Degeneration – from an observed amplitude of the photocenter variation, we cannot separate the components' distance r and the size ratio X .

If P_{orb} is determined and D_1 estimated (from other observations), then the system's semimajor axis r can be constrained using The Third Kepler's Law, assuming a plausible range of bulk densities. Estimating of the size ratio X still largely ambiguous.

Photocenter displacement vs size ratio



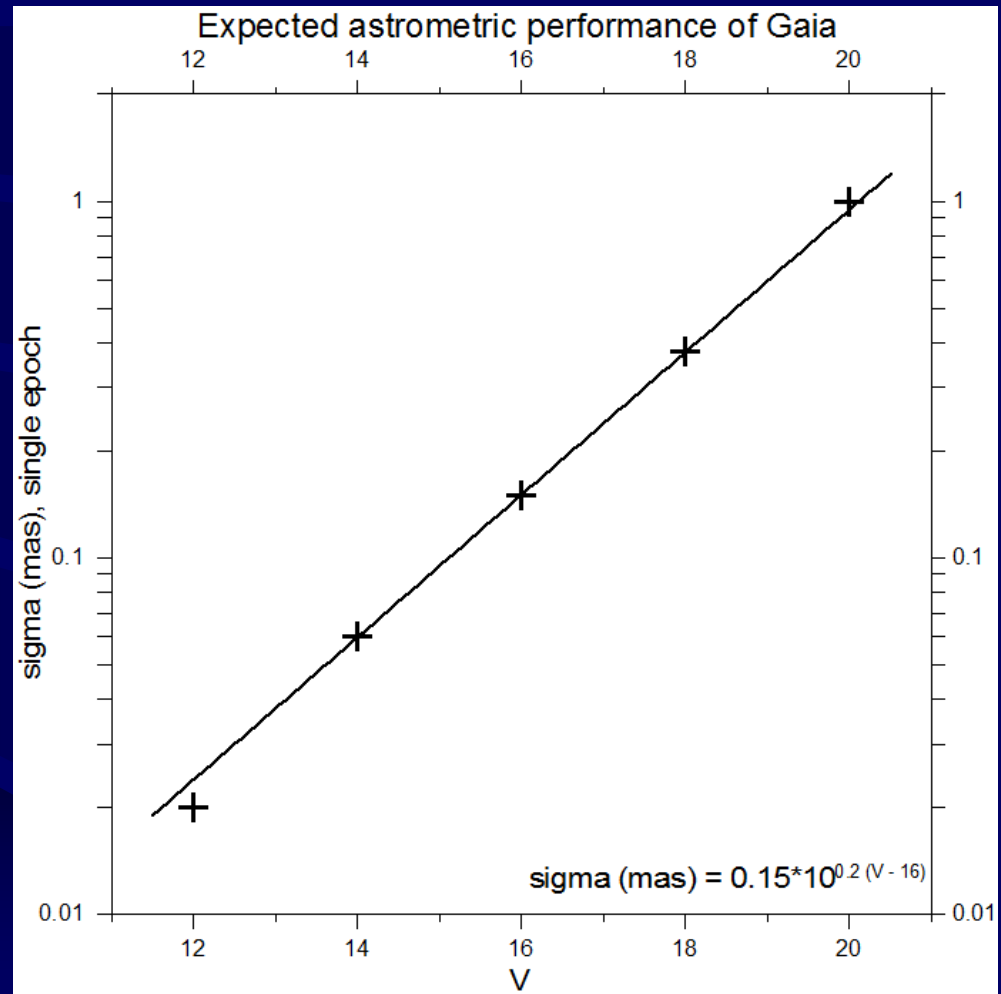
Gaia's expected astrometric accuracy

Single epoch measurement:

V	$\sigma(\text{mas})$
12	0.02
14	0.06
16	0.15
18	0.38
20	1.00

(P. Tanga, pers. comm.)

$$\sigma(\text{mas}) = 0.15 \times 10^{0.2(V-16)}$$



Gaia's performance for NEA and small MBA binaries

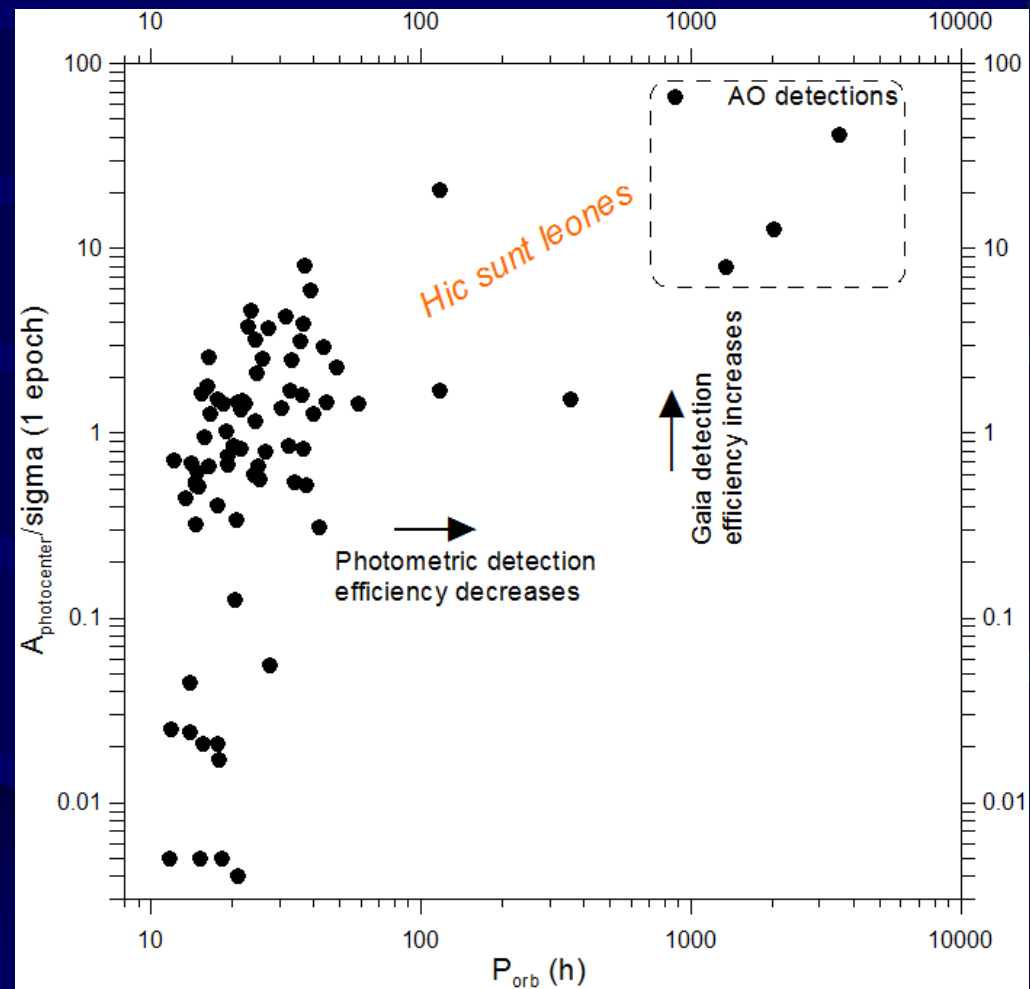
Binary asteroid database
(*Pravec and Harris 2007*, updated).

For each binary, we computed $A_{\text{photocenter}}$ and V at the quadrature (solar elong. 90 deg) and for the mean asteroid's distance from Sun.

$A_{\text{photocenter}}/\sigma(V)$ vs P_{orb} plotted.

Gaia's astrometry noisy for most close binaries: $A_{\text{pc}}/\sigma(V) \sim 1$.

Gaia is promising to describe the population of wider binary systems.



Caveat: Rotational variation of the photocenter in elongated asteroids

For a sphere with the Lommel-Seeliger scattering law, the photocenter is displaced from the projected center of mass by

$$\Delta x \sim R \alpha/3,$$

where Δx is the projected displacement in the sunward direction, α is the solar phase (in radians).

A typical Gaia detected MB asteroid (helioc. dist. ~ 2.5 AU, elong. 90°) has $\alpha \sim 24^\circ$, so $\Delta x \sim 0.14 R$. For $R = 2$ km, the projected displacement is ~ 0.17 mas.

In elongated asteroids, the photocenter displacement varies with rotation.

Prolonged spheroid ($R_b = R_c$) observed at $\alpha = 24^\circ$

$R_a/R_b :$	1.0	1.5	2.0
Photocenter displacement amplitude:	$0.00 R_a$	$0.06 R_a$	$0.09 R_a$
relative to the components separation:	$0.00 a$	$<0.02 a$	$<0.03 a$
(for $a/R_1 > 3$ in known systems)			

An elongated slow-ish rotator could be confused with a close binary with small size ratio that has a similar (low) amplitude of photocenter variation.

Conclusions on Gaia's performance for binary asteroids

Gaia is promising to detect a population of wider binary systems among small MBAs that is almost unknown so far – their components are too close to be resolved with current AO technique, and too distant to be efficiently detected with the photometry method.

Close binary systems (with orbit periods on the order of 1 day), except the largest ones ($D_1 \sim 10$ km, $D_2/D_1 \sim 0.5$), will have noisy signal with $A_{pc}/\sigma(V) \sim 1$ and smaller. Their observations with Gaia may supplement data taken with other techniques.

Possible confusions of elongated slow-ish rotators with close, small size ratio binaries showing a similar (low-amplitude) photocenter variation needs to be investigated.